Journal of the Korean Society
for Nondestructive Testing
Vol. 26, No. 6 (2006. 12)

Detection of Second-Layer Corrosion in Aging Aircraft Fuselage

Nohyu Kim*,† and J. D. Achenbach**

Abstract A Digital X-ray imaging system using Compton backscattering has been developed to obtain a cross-sectional profile and mass loss of corroded lap-splices of aging aircraft from density variation. A slit-type camera was designed to focus on a small scattering volume inside the material, from which the backscattered photons are collected by a collimated scintillator detector for interpretation of material characteristics. The cross section of the lap-joint is scanned by moving the scattering volume through the thickness direction of the specimen. The mass loss of each layer has been estimated from a Compton backscatter A-scan to obtain the thickness of each layer including the aluminum sheet, the corrosion layer and the sealant. Quantitative information such as location and width of planar corrosion in the lap splices of fuselages is obtained by deconvolution using a nonlinear least-square error minimization method(BFGS method). A simple reconstruction model is also introduced to overcome distortion of the Compton backscatter data due to attenuation effects attributed to beam hardening and quantum noise.

Keywords: Layered Corrosion, Digital X-Ray, Compton Effect, Aging Aircraft

1. Introduction

A typical form of corrosion occurring often in aluminum aircraft structures is exfoliative (or layered) corrosion. Exfoliation is a term used to describe a type of corrosion in which takes place parallel to the metal surface. When this occurs, flakes of metal peel or are pushed from the surface due to internal stresses caused by the building up of corrosion products. For a metal to exfoliate a highly directional structure of some sort is required. It is most common in rolled or extruded aluminum alloy products (Al-Cu-Mg and Al-Zn-Mg) such as the aluminum skin in aircraft in which grains are elongated and flattened. Corrosion damage shows three distinct stages. The first represents inter-granular penetration of the recrystalized skin and is slow; the second represents the rapid undermining of the skin as the attack reaches the highly directional material, and the rate is fast; and the third represents the exfoliation attack on the interior structure which proceeds at a rate intermediate between the first and second. Results of constant and spectrum loading fatigue test indicate that the average life is not affected for a slightly exfoliated material but is reduced more than 50 percent for a severely exfoliated material. It is concluded that the existence of exfoliation is a determining factor in fatigue life. That is, the existence of even a small amount of exfoliation can initiate a fatigue crack.

Aluminum corrosion products are amorphous when aluminum corrodes naturally at room temperature. Generally the corrosion products have almost the same or even higher level of electron density as the parent aluminum has. However, studies of aluminum oxide formed on

Received: October 25, 2006, Accepted: November 24, 2006. * Korea University of Technology and Education, Department of Mechatronic Engineering 307 Gajun-Ri, Byungchun-Myun, Chunan 330-860, Korea ** Department of Mechanical Engineering, Northwestern University, Evanston, IL 60208, USA, † Corresponding author: nykim@kut.ac.kr

aluminum show that porosity is needed in order for the corrosion film to grow (Lawson, 1994). This fact is supported by SEM (scanning electron micrograph) of samples of aircraft corrosion products which show them to be porous by an amount of near 50 percent. This porosity is a main contributor to the low electron density, which is proportional to the physical density for a low atomic number material. This is a distinguishing characteristic of corrosion in aging aircraft which is used for corrosion detection by the Compton backscattering technique.

Corrosion is usually found on the entire aircraft after a long period of operation, although most of it is benign. A little metal loss less than 10% is tolerable for the skins of most commercial aircraft. But over 10%, the loss significantly weakens the structure especially when it is combined with crack propagation in the structure. The parts most susceptible to the corrosion in aging aircraft are honeycomb assemblies and fuselages because they provide an easy path and spare for moisture to enter and be trapped inside for a longer time than in other parts. Also water in a honeycomb core or a lap-joint of a fuselage can freeze and expand, subsequently causing failure of the aluminum skin itself or of the adhesive bondline between aluminum skin and the honeycomb core. The main concern of this study is focused on the corrosion of fuselage multi-layered structures of aging aircraft.

A variety of NDE methods have been tried for the purpose of measuring metal loss due to corrosion. The most common and easy inspection technique is visual inspection. The corrosion product in the first skin layer of a fuselage structure shows a swelling made by porosity and corrosion products, so that they can be detected usually. This inspection is clearly valuable, but one cannot expect to detect the forms of corrosion that may be present beyond the first skin layer in a lap joint. Furthermore, if damage is detected, it is important that other tools be used to assess the extent of the corrosion because subsurface damage may be difficult to access quantitatively. One technique which has potential to evaluate aircraft corrosion is the eddy current method. This method works well for measuring the first layer of metal but the sensitivity drops rapidly with depth due to the skin effect. Ultrasonic methods have many advantages for providing one-sided measurements of layered joints, but they require continuity of the structure all the way through because a small air gap blocks the transmission of ultrasonic waves. Air gaps are very common between layers in older aircraft, and even a small air gap blocks ultrasound. Thermal wave imaging is a technique which produces a thermal pattern by thermal waves and can be used to monitor the surface of the part for relatively hot spots caused by blockage of thermal flow away from the surface by a laminar flaw. This method is very sensitive to flaws near the inspection surface but the sensitivity reduces rapidly with flaw depth. Like thermal wave imaging, shearography, a laser holographic technique, can rapidly scan large areas of aircraft skin. But it is limited to the detection of defects or disbonds near the surface.

Traditional transmission x-ray inspection which has been frequently applied for detection of corrosion uses transmitted radiation for imaging purposes and it provide a good image for the corroded area. It is very useful for the detection of honeycomb-core defect in bonded sandwich assemblies. True 3-D information can be obtained at the cost of a significant increase in system complexity, by viewing the object from many different directions, and manipulating the set of projections to reconstruct in some way the spatial distribution of the linear attenuation coefficient (Computer Tomography). It is, however, very limited in real in-situ inspection because the structure should be accessible from both sides, which is generally impossible for airplanes. Compton backscattering permits the placing of the source and the detector on the same side of the object. It provides indications of material-density changes by a change in intensity slope .vs. position and of voids or foreign material by an abrupt change in backscatter intensity (Bssi, 1982 and Harding, 1989). This method is particularly useful for the inspection of laminated structures. For some of these layered structures, ultrasonic inspection approaches are ineffective or impractical, but the backscatter X-ray technique offers a solution.

In this paper, the digital X-ray backscatter system has been developed and applied to layered corrosion of fuselage in aging aircraft to measure the mass loss and location of the corrosion. One-dimensional digital X-ray scan through the thickness of lap-joint was made by focusing the slit-type X-ray beam on scan points which is controlled and moved by scan head. Reconstruction and restoration of raw X-ray data based on nonlinear least square minimization technique are performed to inspect the remaining thickness of aluminum skin of lap-joint quantitatively.

2. Digital X-Ray Depth Profilometry Using Compton Backscattering

Digital X-ray depth profilometry (X-Ray DP) is a digital imaging technique that is developed specifically for the inspection of aircraft structures for corrosion, gives a true cross-sectional view of the object being examined unlike conventional radiographic techniques and CAT scanning which are shadow-casting techniques. Because it is based on backscattering rather than transmission, it can perform inspections of aircraft structures from the outside of the plane without needing access to the interior. X-ray backscatter depth profilometry (X-ray BDP) has been developed to fill the need for an actual thickness measurement of each layer in a multi-layer structure without having to take the structure apart. X-ray BDP is designed to provide a highly accurate depth profile in a location of interest. X-ray BDP eliminates the costly labor and time needed for rivet removal required for direct measurement with calipers. It also eliminates the potential for fatigue crack initiation caused by bending the sheet metal in order to get the calipers in place or make a visual inspection. Point measurement techniques such as X-ray BDP are most needed when there is already some indication that a detailed measurement is desirable. This could be pillowing seen in visual inspection or an indication of corrosion revealed by some other broad-area inspection method such as eddy current scanning, ultrasonic scanning or possibly thermal wave imaging. These methods can detect damage to the first layer or interface disbond and thereby give evidence of corrosion activity. Their strength is in their ability to give a 2-D map of the near sub-surface region quickly. But they have not been able to generate cross-sectional views of much accuracy nor depth profiles. X-ray BDP gives that additional information about thickness which is needed in order to make the decision of whether or not repairs are needed and how soon. What is needed in this type of inspection, what other methods do not readily supply, is information about the thickness of the various layers subject to corrosion. In order to overcome the slowness of full 3- or even 2-dimensional backscatter imaging, X-ray BDP reduces the scan to essentially one dimension. A one-dimensional scan, through the thickness of a layered structure, produces about the same result as would the taking a core sample. But X-ray BDP accomplishes this non-destructively.

To collect backscatter data for corrosion evaluation, the depth-profiling camera, shown in Fig. 1, was developed. The camera consists of X-ray tube (150keV), a radiation detector and sets of precision anisotropic apertures for anisotropic collimation. Significant gains in flux are obtained through the combination of this anisotropy and through optimization of the angles and dimensions used. One pair of apertures, containing one in-plane and one out-of-plane aperture each, along with the focal spot itself, defines the source collimation. A second such pair defines the detector's field of view. The first forms the beam into a pencil with a narrow rectangular cross-section. The second pair of apertures selects a limited-thickness region from which backscattered photons reach the detector. Backscattered photons from the selected scattering zone fall upon a thallium-doped sodium iodide scintillation detector placed outside aperture 4. The intersection of the incident and backscattered beam pencils forms the selected scattering zone. Sweeping this scattering zone through the material to be examined allows visualization along the swept path of the electron density of the material. For aluminum and lighter elements the electron density is equal to a constant times their mass density. The camera is mounted on a positioner that scans it in a direction perpendicular to the surface being examined. The positioner rests against the airplane being inspected. By reducing the scanning to one direction only, the acquisition time for a typical fuselage inspection is reduced to 10 minutes per image. The image may be thought of as being like a density scan plot of a sample core-drilled through the skin. The term "virtual core drill" has been used to describe the X-ray BDP machine for this reason. By selectively spreading the beam, the anisotropy, like the anvil of a micrometer, lets the apparatus

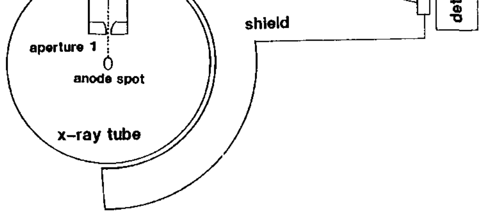

Fig. 1 Compton backscatter camera of X-ray BDP

take particular advantage of the scan's limited dimensionality to obtain higher flux for a given resolution than could be obtained otherwise. The resolution of the X-ray BDP system has been adjusted to measure the thickness of the layers of aircraft skin with an accuracy of about 0.001". This is near to the best accuracy obtainable when measuring the thickness of metal which has not been polished. Manufacturing tolerances, and of course corrosion, both limit the smoothness of real surfaces. Furthermore, surface roughness less than 0.001" is rare for most surfaces on aging aircraft skin layers.

3. Inspection of Corroded Fuselage in Aging Aircraft

After laboratory testing and some preliminary field work, the X-ray BDP apparatus was taken to the FAA/AANC aging aircraft NDI validation center located in Albuquerque, NM, for validation testing. Fig. 2 shows the X-ray BDP being used to inspect a station along a lap splice on a Boeing 737 aircraft located at the FAA/AANC facility. The X-ray BDP unit moves around under its own battery power. The unit is positioned at the point where the scan is to take place, and the scan head shown in Fig. 2(a) is guided to the exact location by an operator. The operator controls the boom and can pivot the scan head. When the scan head is in place, its four foots rest against the plane's surface. Then by operating the boom again, the spring-loaded scan head is pressed against the plane. Friction of the feet against the surface holds the scan head in place. The boom supports the scan head and simultaneously applies pressure to the scan head's feet in whatever position the head may be placed. Fig. 2(b) shows the scan head in position against the side of the airplane. The scan head is thus aligned through its feet against the surface of the plane and largely independent of the motions of the motorized carriage, which transports it. Once in place, the scan head is precisely re-aligned by computer-controlled stepper motors using position sensors which contact the plane and then the scan begins. The computer performs the scan, advancing the motors and stopping at intervals to collect data in the form of X-ray backscattered photon counts. These intervals are usually steps of 0.001" or 0.002". The indications, in a scan, of unexpected low-density material, air gaps and *thinning of metal are the hallmarks of corrosion* in an aircraft sheet metal joint. The presence of loose low density material signals active or untreated corrosion. Air gaps alone, unless greater than a few mils in width, do not by themselves indicate corrosion. But, they do provide good places for corrosion to start. Corrosion products, when compacted, often appear in a scan as material having about half the density of the parent aluminum. Loose corrosion products often have still lower densities. Corrosion products must be porous and the pores are the primary reason that corrosion products are less dense than aluminum. An electron micrograph of undisturbed corrosion product on the surface of a second-layer of skin shows that the relative volume of pores is around 40%.

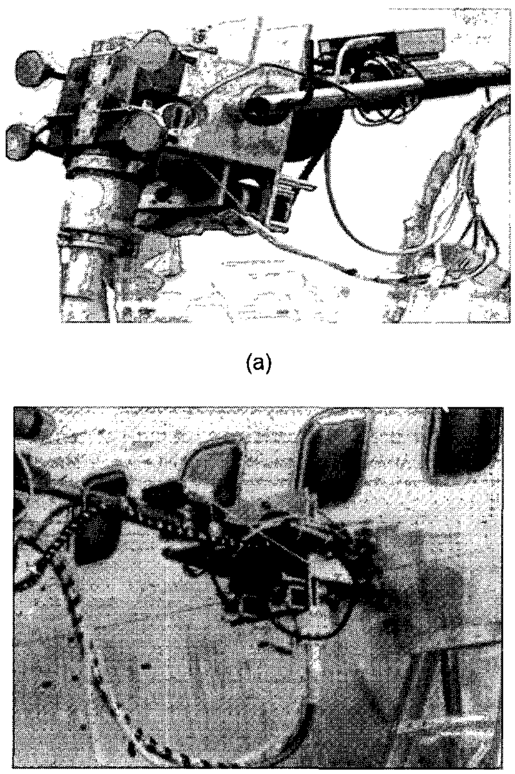

(a)

(b)

Fig. 2 Inspection of B-737 testbed fuselage: (a) scan head; (b) X-ray BDP in operation

During the inspection of Boeing 737 test bed, scatter of X-rays into the environment is an *important issue consideration.* However, the measured radiation level is extremely low, about 0.2 mR/hr, because a very tiny beam is used for Compton backscattering. The radiation level is low enough that, by the standards of most states in USA, namely 2 mRem/hr, operators may safely approach within as little as three feet from the operating X-ray tube.

4. Reconstruction of Digital X-Ray Data

An X-ray beam undergoes many kinds of scattering when it passes through the multi-layered structure, which leads to attenuation of the beam. The rate of attenuation in each layer depends on the mass absorption coefficients of each layer and the energy of the X-ray used. Since the X-ray generated in the X-ray tube has a broad range of energy components like a white light, it is totally incoherent so that each component of an X-ray decays in the material at a different rate which is called "beam hardening". Therefore even though two layers are made of the same material, the attenuation of the X-ray beam in each layer can be different depending on the location of the layers in the structure.

Assuming that the X-ray is monochromatic, the attenuation in a layer in the structure is simply given by

$$I = I_0 \cdot e^{-\mu l} \qquad (1)$$

where, μ is mass absorption coefficient of the layer, l is the distance the beam goes through the layer and I_0 is the intensity of the incident X-ray beam. Then, the restoration of I_0 is easily achieved as

$$I_0 = I \cdot e^{\mu l} \tag{2}$$

Since X-ray beam used in the experimental work is not monochromatic, the mass absorption coefficient μ was determined by curve-fitting the experimental data using equation (1). However, the problem in reconstruction from equation (2) is how to obtain l, the thickness of the layer to be determined from the reconstructed data. In this work, an initial guess for the thicknesses of layers is made and put into deconvolution routine (using the optimization technique) in order to calculate the thicknesses of layers. Then these values are entered again into the reconstruction program which now can provide more accurate restoration of the image. In this manner, errors from guessing the initial thicknesses of layers can be minimized. Fig. 3(a) displays raw scan data taken from a lap joint which shows large attenuation in each layer. Its reconstructed image is Fig. 3(b), where the attenuation in each layer is compensated so well that each layer has a flat-top shape.

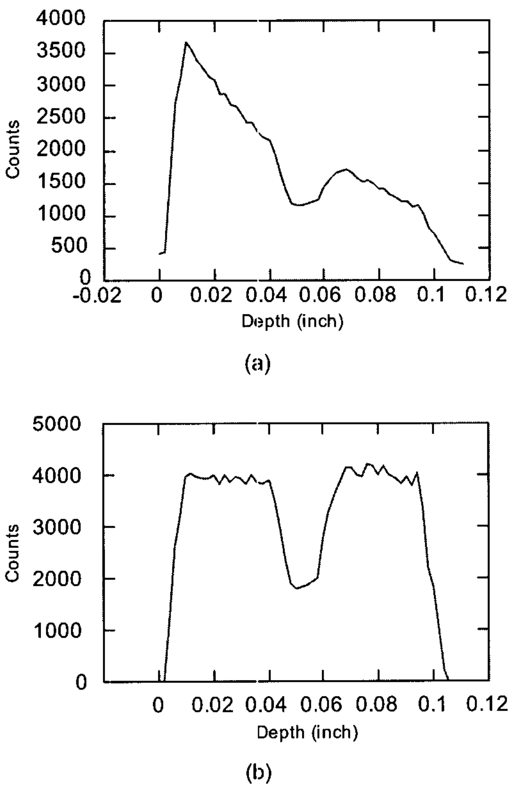

Fig. 3 Reconstruction of raw data: (a) raw X-ray data obtained from a lap joint of the B-737 testbed; (b) reconstructed data

5. Deconvolution and Restoration

5.1 Boltzman Equation for Compton Scattering

Suppose a very well-collimated narrow beam (point source) of intensity I_0 is directed to a point, the origin of the coordinate system. Defining $f(\mathbf{r},\boldsymbol{\omega},\lambda)$ as the photon flux at point vector $\mathbf{r}$ into the direction of $\boldsymbol{\omega}=\eta_x\mathbf{i}+\eta_z\mathbf{j}$ with the wavelength λ, it is determined by the Boltzmann equation as follows (Fernandez, 1989)

$$\begin{aligned}&\boldsymbol{\omega}\cdot\nabla f(\mathbf{r},\boldsymbol{\omega},\lambda)\\&=-\mu(\lambda)f(\mathbf{r},\boldsymbol{\omega},\lambda)+\\&\int_0^\infty\int_{4\pi}k(\boldsymbol{\omega},\lambda,\boldsymbol{\omega}',\lambda')f(\mathbf{r},\boldsymbol{\omega}',\lambda')d\boldsymbol{\omega}'d\lambda'\end{aligned} \tag{3}$$

In equation (3), $\mu(\lambda)$ is mass absorption coefficient and $k(\boldsymbol{\omega}, \lambda, \boldsymbol{\omega}', \lambda')$ is scattering probability function of Klein-Nishina equation. Scattering of photons occurs from any direction $\boldsymbol{\omega}'$ and wavelength λ' into the given direction $\boldsymbol{\omega}$ and wavelength λ. It depends on the product of photon flux $f(\mathrm{r},\boldsymbol{\omega},\lambda)$ and of the probability $k(\boldsymbol{\omega}, \lambda, \boldsymbol{\omega}', \lambda')$ of photon scattering into $\boldsymbol{\omega}$ and λ from $\boldsymbol{\omega}'$ and λ'. In case of normal incidence and monochromatic X-ray, the first-order scattering flux $f^{(1)}(z,\boldsymbol{\omega})$ at a point z in the direction $\boldsymbol{\omega}$ is obtained from the Boltzmann equation as (Mackormick, 1992)

$$f^{(1)}(z,\boldsymbol{\omega}) = I_0 k(\boldsymbol{\omega}) e^{-\mu z G(\omega)} \tag{4}$$

In equation (4), the notation $G(\boldsymbol{\omega})$ is a geometric coefficient for attenuation effect from z to detection point. Even in a layered structure, the equation holds in each layer.

5.2 Optimization for Deconvolution

The optimization technique for deconvolution used in this paper is nonlinear least square minimization method which minimize an error functional defined as the difference between measurement data and theoretical values of equation (4). The iteration proceeds until the functional that represents the goodness of fit is reduced to an acceptably small value. For the case of M data points, we can define a least-square functional Φ depending on the X-ray photon flux $f(z_i,\omega)$ (first order scattering given by equation (4)) measured at point z_i in the direction of ω as

$$\Phi = \frac{1}{2}\sum_{i=1}^{M}\{f^c(z_i,\omega) - f^m(z_i,\omega)\}^2 \qquad (5)$$

where $f^c(z_i,\omega)$ - $f^m(z_i,\omega)$ represents the difference of calculated and the measured values of the scattering intensity function $f(z_i,\omega)$ at z_i. An iterative solution of the inverse problem is obtained by minimizing the value of the functional Φ using BFGS algorithm.

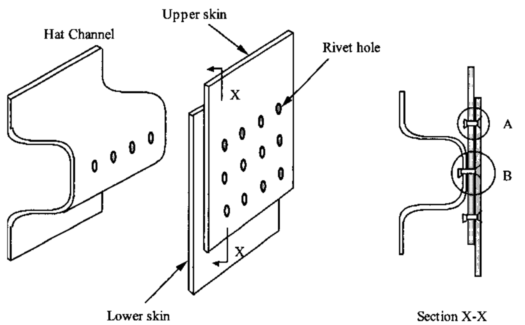

Fig. 4 Lap joint configuration of the B-737 testbed fuselage

6. Results and Discussion

The scans performed between rivets at several points of the lap-splice have been reconstructed and processed through the deconvolution step after reconstruction to obtain the thickness of each layer. The lap-splice of the B-737 testbed fuselage shown in Fig. 2 is composed of three layers, which are the outer skin, the inner skin, and a hat channel as shown in Fig. 4. The outer and inner skins are polished and riveted together to the hat channel. A doubler, a faying strip or a sealant is often inserted either between the two skins or behind the inner skin in order to prevent propagation of fatigue cracks and corrosion. Hence, the scan images taken from different spots on a lap-joint may show two or three sometimes four/five layers depending on the scan point on the lap-joint. Fig. 4 shows that typical scan points are in one of the two regions of the lap-joint, one of which is region A where only two skins can be seen with or without a sealant or a doubler between them. The other one is region B where a structural element such as a stringer or a longeron is detected behind the two aluminum sheets.

The dotted line in Fig. 5(a) is a reconstructed scan obtained from region A, where only two aluminum sheets appear, but between them exists a low density material which may be a bonding resin or a corrosion product. The solid line in Fig. 5(a) represents the curve-fitting result of a reconstructed image(dotted line) using the BFGS method when an air gap is assumed to exist between the two aluminum skins. The curve-fitting is quite good except in the region of low density material between the two aluminum layers. The big difference between the two curves in that region means that the assumption is wrong, i.e. the valley in Fig. 5(a) is not an air gap but something else with low density. In Fig. 5(b) where a low density material is assumed between the two skins, the reconstructed image (dotted line) very well fits over the whole range. Therefore, it may be concluded that the low density material is a resin bond or a corrosion product trapped between the skins, or both of them. Through deconvolution using the BFGS method, the thickness of each layer has been calculated. The results are displayed in Fig. 5(c) and 5(d). Fig. 6 is another scan taken at the

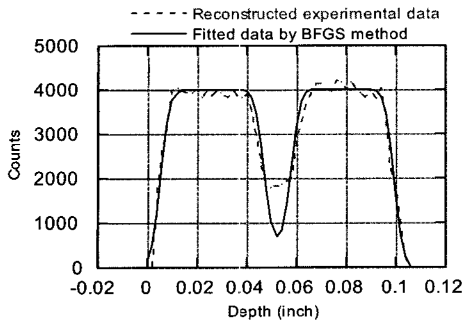

(a)

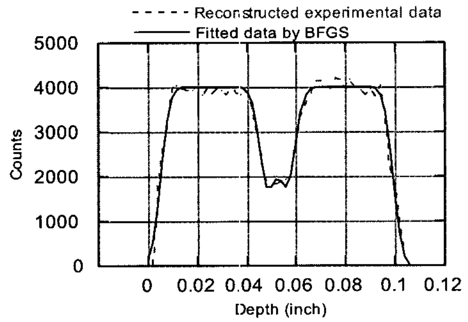

(b)

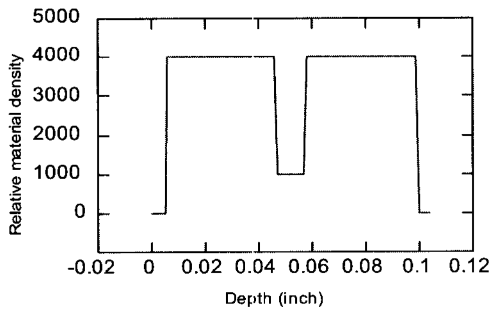

(c)

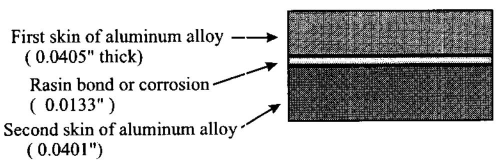

(d)

Fig. 5 Reconstruction and deconvolution of scan data in region A: (a) reconstructed data and curve-fitted data by BFGS method when the second layer is assumed to be an air gap; (b) reconstructed data and curve-fitted data by BFGS method when the second layer is assumed as a low density material; (c) restored data; (d) thickness of layers

region A with a faying strip or sealant between the two aluminum skins. In Fig. 6(b) and 6(c), there are clear disbonds between the aluminum skin and the faying layer which strongly imply the development of corrosion inside the gap. The back surface of the lower aluminum skin seems to be painted because the slope of the dotted curve at the back surface in Fig. 6(a) is a little bit lower than that of the curve-fitted line (solid).

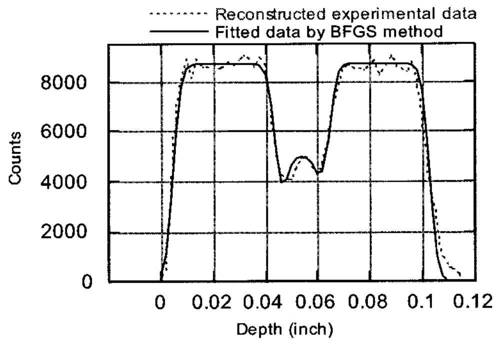

(a)

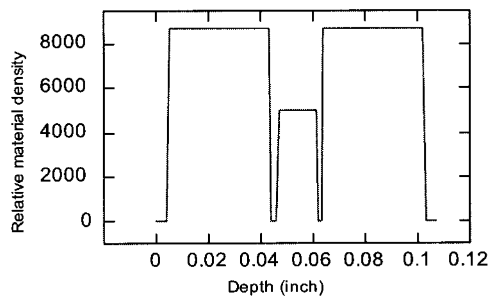

(b)

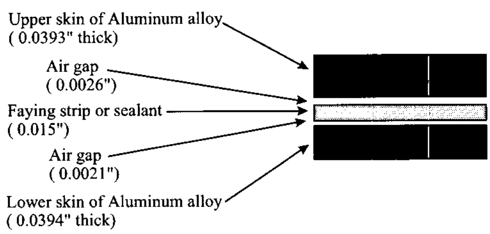

(c)

Fig. 6 Restoration and deconvolution of X-ray scan data from a lap-joint in region A: (a) reconstructed data and curve-fitted data by BFGS method; (b) deconvolved data; (c) thickness of layers

The scans in Fig. 7 and 8 were conducted in the region B where three layers were detected. A faying strip and a sealant between the first and the second skin in Fig. 7 is totally detached from both skins leaving a wide air gap which probably indicates the presence of corrosion. The rear surface of the second skin is very irregular which is caused by severe exfoliative corrosion of the surface. It appears in Fig. 7(a) as a very low density material. The third layer is a stringer that seems to be covered with a thick layer of paint on the back surface because the slope of the rear surface is lower than the curve-fitted slope(solid line). The front side of the stringer has also a low slope, which means that it is either corroded or painted. It measured only 0.0326" in thickness. Examination within the plane showed that the stringer was indeed this thick at points near where the scan was taken. The last scan from region B is shown in Fig. 8, where apparently two air gaps exist between the layers. The thicknesses of the layers are displayed in Fig. 8(c).

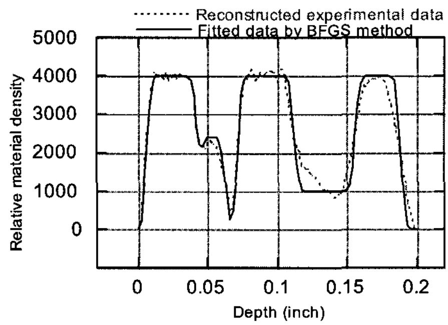

(a)

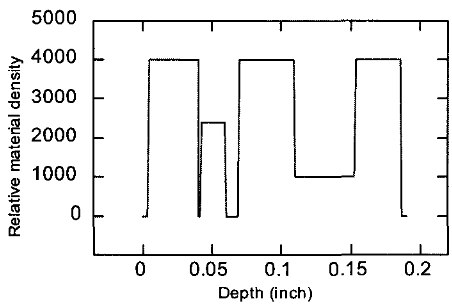

(b)

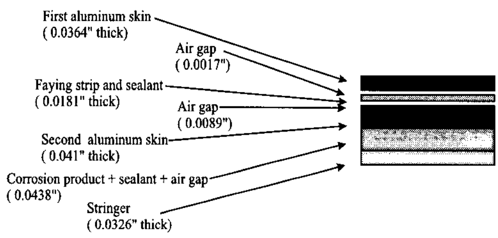

(c)

Fig. 7 Restoration and deconvolution of X-ray scan data from a corroded lap-joint in region B: (a) reconstructed data and curve-fitted data by BFGS method; (b) deconvolved data; (c) thickness of layers

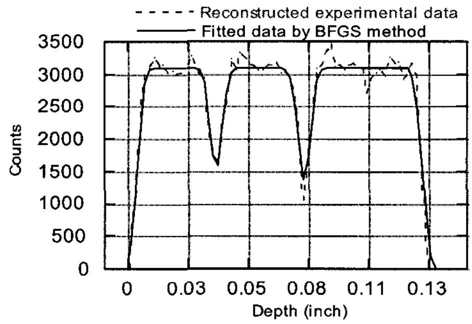

(a)

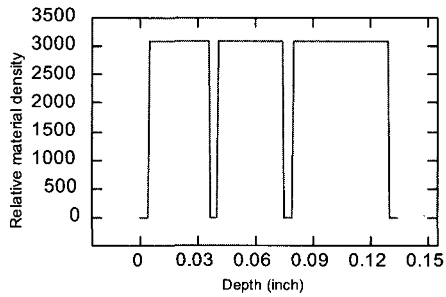

(b)

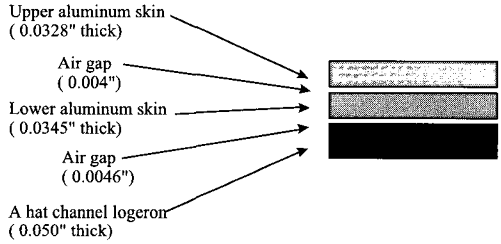

(c)

Fig. 8 Restoration and deconvolution of X-ray scan data from a relatively sound lap-joint in region B: (a) reconstructed data and curve fitted data by BFGS method; (b) deconvolved data; (c) thickness of layers

7. Conclusions

Digital X-ray technique using the Compton backscattering was applied to the detection of second layer corrosion in lap-joints on a Boeing 737 airplane located at the FAA/AANC facility. The X-ray depth profilometry (DP) operating under its own battery power is developed and used to inspect several points of lap-spice on the fuselage where the scan is made through the thickness. Even though the fuselage surface was very rough and uneven, the scans were successfully conducted by the Compton backscattering imaging system. Since corrosion products tend to peel off from the corroded sheet metal, an unexpected low density material or thinning of metal was found as a clear indication of corrosion in the sheet metal joint. Mass loss was evaluated by measuring the remaining thicknesses of the aluminum skins based on the reconstruction and deconvolution of raw digital data. From the experimental data of this study, following conclusions can be drawn.

1) The Compton backscattering technique is proved particularly useful for one-sided inspection of radiographically thin structures such as aluminum sheet of aircraft fuselage.

2) Detection of exfoliative corrosion in second layer aluminum alloy sheets is made possible not by the corrosion product itself, but by the porosity formed inside the corrosion product.

3) The radiation hazard in the field is low enough to meet U.S. regulations; less than 0.2mR/hr at operator's position (10 feet from the source).

4) Restored corrosion data in lap-joint of the fuselage determined by nonlinear least square error minimization technique show that the most severe corrosion occurs between the first and second aluminum skin.

References

Bssi, H., Friddell, K. D., and Nelson, J. M. (1988) Backscatter X-Ray Imaging, Materials Evaluation 46, pp. 1462-1465

Fernandez, J. E. (1989) XRF Intensity in the Frame of the Transport Theory, Nuclear Instruments and Methods of Physical Research, A 280, pp. 212-221

Harding, G. and Kosanetzky, J. (1989) Scattered X-Ray Beam Nondestructive Testing, Nuclear Instr. and Methods, A280, pp. 517-523

Lawson, L., N. Kim (1994) Deconvolution and Detectability in Compton Backscatter Profilometry, Review of Progress in Quantitative Non-Destructive Evaluation, Vol. 13b, pp. 1971-1978

Mackormick, J. (1992) Inverse Radiative Transfer problems: A Review, Nuclear Science and Engineering, 112, pp. 185-198